Emission impacts of supply chain disruptions for COVID and China's solid waste import ban

John Ryter
MIT https://orcid.org/0000-0002-0343-7553
Xinkai Fu
MIT
Karan Bhuwalka
MIT
Richard Roth
MIT
Elsa Olivetti (elsao@mit.edu)
Massachusetts Institute of Technology https://orcid.org/0000-0002-8043-2385

Article

Keywords:

Posted Date: November 19th, 2020

DOI: https://doi.org/10.21203/rs.3.rs-86991/v1

Version of Record: A version of this preprint was published at Nature Communications on June 18th, 2021. See the published version at https://doi.org/10.1038/s41467-021-23874-7.

Abstract

Climate change will increase the frequency and severity of supply-chain disruptions and large-scale economic crises, also prompting environmentally-protective local policies. Here we use econometric time series analysis, inventory-driven price formation, dynamic material flow analysis, and gate-to-gate life cycle analysis to model the response of each copper supply chain actor to China's solid waste import ban and the COVID-19 pandemic. We demonstrate that the economic changes associated with China's solid waste import ban increase primary refining within China, offsetting the environmental benefits of decreased copper scrap refining and generating a cumulative increase in CO2e emissions of up to 35 Mt by 2040. Increasing China's refined copper imports reverses this trend, decreasing CO2e emissions both in China (up to 300 Mt by 2040) and globally (up to 63 Mt). We test model outcome sensitivity to supply chain disruptions and economic crises using GDP, mining, and refining shocks associated with the COVID-19 pandemic, showing the results maintain impact magnitude alongside disruption effects.

Introduction

The transition toward a zero-carbon society is coupled with increasing electrification, prompting projections that demand for copper, the third most-consumed metal, will increase by more than 300% and consume 2.5% of the world's energy by 2050, with greater increases under more equitable global development scenarios.[1] At the same time, copper ore grades continue to decline and extraction operations are increasingly concentrated in low-income regions with decreased enforcement of best practices.[2,3] These regions are also expected to experience the most intense effects of climate change,[4] and copper resources in particular are concentrated in areas of high water scarcity risk.[5] These conflicting goals necessitate an integrated assessment of the copper material system and further emphasize the need for recycling and other resource efficiency principles in this supply chain.[6]

In an effort to address air pollution and limit soil and water toxicity while maintaining economic progress, China has implemented resource efficiency policies centering the circular economy as a national development strategy.[7,8] While much of this legislation has garnered broad international support and improved local health outcomes,[9,10] China's Green Fence (2013) and National Sword (2017) policies, which restrict nearly all solid waste imports, have also caused disruption across a variety of supply chains and led to increased landfilling and buildup of recyclables in high-income, waste-exporting countries.[8,9,11,12] Chinese companies facing consequent scrap supply shortages have reinvested in recycling facilities throughout Southeast Asia, Australia, and the United States,[13-15] indicating a redistribution of scrap processing environmental impacts.[16]

Studies to date have emphasized the ban's impact on plastic waste streams, primarily addressing geographical redistribution, increased landfilling, and environmental impacts.[8,12,17,18] Several authors have shown that China's domestic secondary copper supply is insufficient to meet its increasing metals demand, where Zeng et al., Wang et al., and Dong et al. explicitly account for changes in scrap imports.[19-22] With prior studies relying primarily on top-down material flow analyses, a significant research gap remains in understanding supply-chain reactions stemming from the solid waste import ban, the ban's resulting environmental impacts, and mechanisms for maximizing environmental benefits in China and globally.

The COVID-19 pandemic has introduced a supply chain shock alongside the solid waste import ban. Macroeconomic effects have decreased global copper demand,[23-25] while recent outbreaks have increased death among miners and halted production at some of the world's largest copper mines, reduced refinery production, and limited scrap trade.[26,27] Simultaneous demand rebound in China is expected to produce supply deficits and price increases in 2021.[26,28] Relevant recent studies have addressed pandemic effects at the macroeconomic level, emphasizing short-term effects, and have been unable to comment on medium- to long-term impacts on individual supply chains, the impacts of combined supply-demand shocks, or external policy resilience to these shocks.[29-31]

This study uses econometric time series analysis, inventory-driven price formation, dynamic material flow analysis (dMFA), and life cycle analysis (LCA) to estimate copper supply chain and environmental impact evolution under differing regional policy change and global economic shock scenarios.[32] The model architecture differentiates supply chain behavior between China and the rest of the world and considers differences in scrap composition, availability, and price in those two regions. We estimate the evolution of cathode and scrap prices, refinery processing fees (treatment and refining charges, TCRC), and production and consumption of copper scrap, concentrate, and refined material through 2040, primarily reporting results as cumulative departure from baseline.

Results

Current Impacts of the China Solid Waste Import Ban

China's solid waste legislation includes the National Sword policy at the beginning of 2017, the ban of Category 7 copper scrap in April 2017, the imposition of tariffs on US copper scrap imports in August 2018, and the additional restrictions on Category 6 copper scrap imports in December 2018. These policies have produced a redistribution of copper scrap trade and compositional changes in China's scrap imports (Figure 2a). The gross weight of China's copper imports has declined over the last several years, with a corresponding increase in copper fraction producing a near-constant copper content by mass. These data reflect the success of China's policy goal of decreasing low-grade scrap imports and processing, and coincide with the redistribution of global scrap trade and processing.

According to industry experts, Rep. of Korea, India, Germany, Taiwan, Belgium, Malaysia, Canada, and Vietnam have begun importing the majority of this newly-available low-grade scrap, with some fraction simply being upgraded and re-exported to China (Supplementary Tables S8-S9).[13,14] This behavior is particularly evident in Rep. of Korea, Taiwan, Malaysia, Canada, and Indonesia; these regions have dramatically increased both copper scrap exports to China and copper scrap imports (Figure 2b). Simultaneously, US gross weight copper scrap exports to China fell from 68% to 10% from 2017 to 2019, while the fraction of EU copper scrap exports to China fell from 29% to 15% in the same period. While the copper fraction of China's copper scrap imports nearly doubled from 2017 to 2019, within Indonesia, India, and Malaysia this value decreased 10%, 15%, and 39% respectively, indicating more contaminated scrap streams. For the remaining nations listed above, the copper fraction of copper scrap imports changed no more than 5% over this period.

Future Impacts of the China Solid Waste Import Ban

We simulate projected import restrictions for cases where scrap with less than 94 or 99% copper content would not be permitted for import. Such restrictions would eliminate imports of alloyed scrap grades, No.2 scrap, or both, with <99% copper content restricted and only No.1 copper scrap (ISRI grade Barley) permitted to enter China.[33,34] We analyze scrap import reductions of 50% year over year for each category with ±25% as sensitivity while other imports remain constant (Figure 3a). Following China's reclassification of copper scrap to recycled copper or brass solid waste material on July 1, 2020, the No.2 ban scenario approximates reality; industry experts predict free trade of high-quality recycled copper and brass raw materials and consequent policy stability in the near future.[35] We provide additional granularity surrounding the No.2 scrap ban scenario.

In effort to highlight relative changes, results are presented as the cumulative departure from the baseline scenario as a percentage of the projected 2020 value for that parameter; absolute responses (in thousand metric tonnes) may be found in Supplementary Figures S5-S7. The solid waste import ban shifts scrap availability from China to RoW, increasing prices in China and decreasing prices for RoW, prompting a redistribution of primary and secondary refining production (Figure 3b). Due to time delays and differing magnitudes of scrap availability shifts, the decrease in RoW primary refining and increase in RoW secondary refining lag the opposing responses in China, producing a global increase in primary refining production and decrease in secondary refining production (Figure 3d). Increasing scrap demand in RoW is unable to offset the increasing prices and decreasing demand in China, generating a net decrease in global scrap demand (Figure 3d). Resulting changes in cathode price are insufficient to drive a significant departure from baseline and the small increases in mining and primary refining production are erased by market corrections by 2040. While scrap consumption appears approximately linear as a function of scrap quantity restricted, the No.2 ban generates a larger system response than the ban on alloyed scraps for refining, mining, and CO_2e emissions responses (Figure 3e).

Global parameters either decrease or remain effectively unchanged relative to baseline by 2040, leading to the expectation of negligible changes in environmental impacts. However, the redistribution of primary and secondary refining between China and RoW, coupled with higher unit impacts of Chinese primary refining, produces an increase in global CO_2e emissions of 18 Mt, or 7.1% of current annual emissions due to copper production (Figure 3c). This result corresponds with an 28% (31 Mt, 12% of global) increase in CO_2e emissions from copper within China, equivalent to the annual CO_2 emissions of 6.6 million gasoline vehicles.[36] This large emissions increase is the result of increased primary refining production, while the decreases in scrap use and fabrication account for the smaller contributions toward decreasing emissions (Figure 3f). Increasing primary refining production requires increased concentrate imports – determined endogenously – due to limited domestic copper ore bodies, continuing the present logistic growth trend (Supplementary Figure S3).

All 12 environmental impact indicators considered in this study follow similar trends as the CO_2e emissions response (Supplementary Figures S8-S9). Given the pollution reduction goal of China's solid waste policies, smog-, respiratory-, and human toxicity-related emissions are of particular importance and these results show 28% (5.4 Mt O_3 eq), 45% (45 kt PM2.5 eq), and 36% (1200 comparative human toxicity units, CTUh) increases above the baseline 2020 value within China. Without further action, economic responses to this policy will produce unintended negative environmental consequences.

Responding to the China Solid Waste Import Ban

Higher Chinese refined copper imports may mitigate the effects of the scrap ban and take advantage of the newly-available scrap available outside China, and correspond with some of China's foreign investment strategies to date.[8,14,15,37] We increase or decrease China's refined copper imports at rates of 100 or 200 kt/year (Figure 4a) coincident with the No.2 scrap ban. We assumed that China would not begin exporting refined copper and the minimum value was set to zero. We show that increasing China's refined copper imports redistributes both primary and secondary refining production from China to RoW by shifting regional refined copper demand (Figure 4c). Globally, this shift enables better use of displaced scrap material (cumulative 10% of 2020 value, 1.0 Mt), resulting in increased secondary refining (6.4%, 1.3 Mt), decreased primary refining (6.3%, 1.3 Mt), and decreased mining production (5.9%, 1.2 Mt; Figure 4b).

This global decrease in primary refining and mining production (Figure 4b), coupled with the redistribution of refining from China to RoW (Figure 4c), enables a cumulative global reduction in CO_2e emissions equal to 25% of 2020 emissions due to copper production. This value exceeds that of the mining reduction alone due to the differences in unit environmental impacts of refining within China and the global average. Within China, CO_2e emissions decrease a cumulative 270% (300 Mt or 120% of global) of the estimated 2020 emissions in China by 2040, smog-related emissions decrease 240% (46

Mt O_3 eq.), respiratory-related emissions decrease 260% (2.6 Mt PM 2.5 eq.), and human toxicity-related emissions decrease 240% (8000 CTUh).

Decreasing China's refined copper imports represents a continuation of the 2015-2018 trend, while increasing imports represents the case where China acts to redistribute primary refining activities outside its borders alongside scrap refining activities. Further decreasing China's refined copper imports exacerbates the negative effects of the scrap ban by causing China to increase refining further still, while reversing that trend produces environmental benefits both within China and globally. Increasing China's refined copper imports does, however, increase environmental impacts for RoW. While much of the redistribution to date has been to regions with reduced environmental regulations, these localized impacts can be minimized if smelting and refining investment prioritizes regions and technologies with better environmental practices. The relative inelasticity of total refining production, the nearly equal and opposite changes in global mining production, and scrap consumption stemming from increasing China's refined copper imports indicate a market-stable transition in the direction of a circular economy, and at minimum lower unit emissions for the copper material system (Figure 4b).

Sensitivity to Supply Chain Disruptions

To understand how these policies evolve in the face of future climate- and social unrest-induced supply chain disruptions, we simulate the impact of major system shocks using production and consumption changes stemming from the COVID-19 pandemic. We use 2019-2021 GDP changes from the International Monetary Fund (Figure 5a),[38] and calculate copper demand endogenously from GDP per capita evolution (Figure 5b). We account for operational discontinuities by adjusting mine capacity utilization, refinery capacity utilization, and refinery secondary ratio (the fraction of secondary material used in secondary refineries) for 2020 according to data from the International Copper Study Group. We use mean year over year changes from the first 5 months of 2019 and 2020 ±50%, producing large, moderate, and small responses for each of these four parameters. The annual timescale of this model necessitates that evolution of copper price and other market indicators begins in 2021, the year following the shock.

In testing supply chain resilience to such shocks, we found a reduction in cumulative total refining production (Figure 5c), indicating that post-shock recovery effects may not sufficiently compensate for short-term production disruption. Demand rebound prompts a period of high copper cathode prices, incentivizing mining and primary refining production at the expense of scrap consumption and secondary refining production (Figure 5c). China exhibits a more muted CO_2e emission response due to its more limited GDP growth reductions and low fraction of global mining production, with the bulk of China and RoW declines attributable to manufacturing contraction (Figure 5d). Among small GDP shocks, incorporating larger mine and refinery shocks generates CO_2e emissions reductions equivalent to those of large GDP shocks (Figure 5e). Further analysis has shown that these reductions stem from the secondary ratio shock specifically (Supplementary Figures S14-S15). This shock produces an increase in primary refining production leads to a concentrate supply deficit, mine overproduction, and eventually a price collapse that promotes mine closure and delays mine opening[39,40] while limiting secondary refining recovery. Changes in GDP per capita dominate the long-term system response, with mine and refinery production disruptions producing small but non-negligible changes and secondary ratio changes dominating for sufficiently small GDP shocks.

Incorporating these supply chain shocks immediately following the No.2 scrap ban generates combined effects approximating the sum of the independent responses. Relative to the no-ban scenario described above, secondary refining production decreases while primary refining production increases or remains constant due to time lag effects associated with China-RoW refining redistribution. These changes lead to increases in cumulative mean CO_2e emissions of 7.4 to 17 Mt (2.9 to 6.7% of the 2020 value) relative to the supply chain shock-centered responses, nearing the 18 Mt value without supply chain shocks. Within China, mean emissions increase 26 to 32 Mt (10 to 13% of global 2020 value, 24 to 30% of China 2020 value) relative to the supply chain shock-centered scenarios, overlapping the 31 Mt increase in the no-shock scenarios above. Relative to baseline, mean emissions increase in China by up to 32 Mt, while a decrease in emissions (5.4 Mt) is only maintained for the largest GDP and secondary refining disruptions investigated. These results indicate that, within China, the environmental benefits stemming from these supply chain disruptions are insufficient to offset the increasing emissions resulting from the solid waste import ban for all but the largest economic and trade disruptions.

When refined copper import changes are coincident with the solid waste import ban and supply-chain disruptions, we again observe a redistribution of primary and secondary refining. These changes result in decreased primary refining and mining production, increased secondary refining and scrap consumption, and near-constant total refining production indicating a decrease in copper system unit impacts amid business-as-usual demand growth following the shock. For a large increase in China's refined copper imports (+200 kt/year), mean global CO_2e emissions decrease a cumulative 65 to 73 Mt (26 to 29% of 2020 value) relative to supply chain shocks alone (compare with 63 Mt decrease without supply chain shocks above), or 73 to 150 Mt relative to baseline, doubling even the largest shock-induced emissions reductions. These impact reductions are concentrated within China, with China's cumulative CO_2e emissions decreasing 300 Mt (120% of global 2020 value, 270% of China 2020 value) relative to supply chain shocks alone or 300 to 330 Mt relative to baseline (64 to 72 million vehicles).

For both the scrap and refined copper import policies explored here, their modeled impacts manifest as an approximately additive effect when combined with the supply chain disruption scenarios. The modeled responses therefore remain valid for large-scale supply chain shocks, including those that vary in regional severity, given that the GDP per capita shock is more intense in RoW than in China. Large supply chain shocks such as those associated with the COVID-19 pandemic may partially mask the environmental impacts associated with the solid waste import ban, but it will not erase them, and a redistribution of primary refining activity to outside China remains a viable mechanism for mitigating these effects. Under circumstances where these shocks produce additional restrictions on environmentally-harmful industries,[25] environmental impact reductions beyond those shown here may occur.

Conclusion

China's solid waste import ban has induced a shift in the location of scrap processing, with Malaysia and other Southeast Asian nations accounting for the majority of recent scrap processing investment (Figure

2b). Zeng,[19] Dong,[22] Eheliyagoda,[41] Liu,[42] and Wang[20] show that China's domestic copper scrap generation cannot meet its increasing raw material demand and we confirm these results, demonstrating that the solid waste import ban results in increased primary refining and concentrate imports within China to account for refineries' loss of secondary material. The solid waste import ban's impacts on scrap availability, and consequently price, drive a redistribution of primary refining from RoW to China and of secondary refining from China to RoW. The RoW response rate keeps the redistribution of refining activities from being even and proportional, and secondary refining is projected to decrease globally. Even as Chinese scrap- and manufacturing-related emissions decrease, China's increasing primary refining production more than offsets these benefits (Figure 3f) and generates a net increase in environmental impacts by 2040 across all impact categories considered in this study, both in China and globally.

Increasing China's refined copper imports acts to mitigate these effects and capitalizes on the newly-available scrap available outside China (Figure 4b), mirroring some of China's current foreign investment strategies.[8,14,15,37] The nearly equal and opposite changes in global mining production and scrap consumption indicate a market-stable transition toward a circular economy and lower unit emissions for the copper material system. Given their compositional similarities and that this study includes smelting within refining processes, model results would be similar for increased imports of copper blister, anode, or fabricated products.[43] Potential mechanisms for increasing imports of these materials therefore include limiting China's concentrate imports below 10 Mt (see Supplementary Figure S3), increasing China's copper imports above 2018 levels, and prioritizing investment in recycling, mining, refining, and fabrication technologies with high environmental standards.

Such policy acts to reverse the current trend of outsourcing polluting industries to lower-income regions. While economy-scale analyses provide evidence for the environmental Kuznets curve – that per-capita emissions follow an inverted U-shaped trajectory as per-capita income increases – accounting for trade has been shown to produce a linearly-increasing curve instead.[44] Our results provide the first system-level evidence supporting these conclusions. When increasing China's refined copper imports, 80% of the emissions reduction within China is redistributed to RoW, generating a net global decrease in emissions due to economic effects and lower unit impacts in RoW. This value is consequently dependent on the relative environmental impacts of industrial activities for each trade partner, explicitly demonstrating that nations' environmental impact reductions may be directly accomplished via outsourcing.

Our analysis of large-scale economic and supply chain shocks shows that the long-term environmental impacts of the solid waste import ban and refined copper import policies remain valid even with disruptions in mining and refining production. Elevated sensitivity exists for changes in GDP growth and refinery secondary ratio, where GDP growth shocks dominate at high values. We also show that the impacts of policies such as the China solid waste import ban and increasing China's refined copper imports translate approximately linearly onto such shocks, indicating the results of these policies are robust in the face of supply chain disruption.

Methods

Model Framework

The copper material system model developed by Dr. Xinkai Fu formed the basis of this model.[32] The production and consumption of four material stages within the copper system – ore, scrap, refined copper cathode, and semi-fabricated goods – were modeled based on MFA and inventory-driven price formation, where econometric time series analysis of historical data was used to determine the price, production, and consumption responses that minimize supply-demand imbalances for each material stage. As such, the original model flow can be characterized as follows, starting from model initialization in 2018 with iteration on an annual basis through 2040:

1. Cathode price, treatment and refining charges (TCRC), and scrap spreads (differences between scrap and cathode prices) are determined based on supply-demand imbalances from the previous year;
2. Mines respond to the market state by altering their capacity utilization, opening, or closing;
3. Total copper demand is estimated based on exogenous GDP per capita and sectoral (e.g. construction, automotive, or industrial) volume projections, coupled with copper intensity (kg Cu per kg product) response to price, as developed from collaborator Karan Bhuwalka;[45]
4. Primary and secondary refinery production are estimated based on TCRC and No.2 (ISRI code Birch) scrap spread;
5. Post-consumer (old) and post-industrial (new) scrap supply are estimated using standard MFA procedure, using previous years' demand values, lognormal sectoral product lifetimes, and estimated scrap collection rates, technical recycling efficiencies, and home and exchange scrap ratios from Glöser et al. and SMM;[46,47]
6. Refined copper and direct melt scrap consumption are estimated based on the prior demand prediction, the ratio between alloyed and unalloyed copper products, and scrap conversion efficiencies.

Several components required further development to enable regional and scrap composition considerations for system evolution under the China solid waste import ban. The prior global model was separated into two co-evolving components – China and the rest of the world (RoW) – where the distribution of refined and scrap material consumption between these regions was determined by a linear programming optimization model. For this optimization model to operate, additional granularity surrounding semi-fabricator compositional requirements and scrap composition, availability, and demand were required. Each of these model expansions is explained below, while the model base is described in Dr. Fu's doctoral thesis.[32] A gate-to-gate life cycle analysis was performed using the production data resulting from scenario analysis.

Regional Evolution

Historical values for production and consumption both in China and globally were compiled from data provided by the International Copper Study Group (ICSG),[48,49] the International Copper Association (ICA), Minsur, Glöser et al at Fraunhofer ISI,[46] the International Wrought Copper Council (IWCC),[50] CRU Group, S&P Global Market Intelligence,[51] Wood Mackenzie, the Shanghai Metals Market, American Metal Market, and UN Comtrade (Supplementary Table S1 for full list of data sources).[52]

In developing the China-RoW regional model, cathode prices, TCRC, and mining evolution were assumed to behave as global parameters due to market liquidity, while scrap spreads, copper demand, primary and secondary refined copper production and consumption, and scrap production and consumption required regionalization. China's scrap and refined copper imports were specified as exogenous variables, while concentrate imports were implicit in regional refinery operation. Scrap spreads evolve as a function of the scrap supply-demand balance and the change in cathode price, and scrap spread elasticities to changes in these values retained their global values from the previous model. However, scrap spreads were modeled at the regional level to enable changes in regional scrap availability to impact scrap consumption, and thus regional refinery evolution. The deviation of China and RoW scrap prices from the calculated global values was further explored as a model sensitivity as discussed in Supplementary Methods: Sensitivity to Scrap SD Elasticities. Total copper demand was previously calculated by region[32] – China, EU, Japan, North America, and other – and was simply regrouped to reflect the China-RoW split.

Global refinery production was previously modeled as two individual refineries representing primary and secondary refineries, where primary refineries consume only primary material and secondary refineries consume some fraction of secondary material. In secondary refineries, the secondary ratio (SR) describes the secondary fraction of total raw material consumed. In regionalizing refinery production, the two representative refineries were further split to emulate China and RoW primary and secondary refinery production. Each refinery's capacity evolved as a function of regional copper cathode demand, with long-run capacity elasticity to demand remaining the prior global value. Similarly, primary and secondary refinery capacity utilization (CU) elasticities to TCRC, as well as SR elasticities to TCRC and No.2 scrap spread, retained their global values. Initial values for regional primary and secondary CU and SR were estimated based on individual refinery data from Wood Mackenzie grouped by region, and refinery capacity was calculated such that each representative refinery's production matched 2018 regional production values based on these parameters. These methods are further elaborated in Supplementary Section A1. Refinery raw material consumption was calculated assuming concentrate to cathode and No.2 scrap to cathode efficiencies of 99%. Regional cathode consumption was calculated using the combined blending model described below.

Copper-Based Product Fabrication

As in the previous, less granular model, global copper demand is estimated as the product of regional (China, EU, Japan, North America, and other) and sectoral (construction, electrical, industrial, consumer and others, and transportation) volume and intensity values. Regional sectoral volumes – e.g. total mass of all materials consumed in China's construction sector – are projected through 2040 as in Dr. Fu's thesis,[32] and are static and exogenous to the model. Regional sectoral usage intensities define the copper mass per mass of material in each region and sector, and are determined endogenously based on copper price and exogenous GDP per capita to allow for dematerialization, substitution, and income effects. Bayesian regression models were used to estimate the parameters in this model, shown below, as described by Bhuwalka et al.[45]

$$\Delta log\left(I_{s_i,r_j,t}\right) = \beta_{0,s_i} + \beta_{s_i}\,\Delta log(P_t') + \beta_{r_j}\,\Delta log(P_t') + \beta_{GDP}\,\Delta log\left(GDP_{r_j,t}\right) \tag{1}$$

Where each sector, s_i, and region, r_j, has copper use intensity at time t represented by $I_{s_i,r_j,t}$, which is a function of a sector-specific intercept β_{0,s_i} representing dematerialization, sector- and region-specific copper price coefficients β_{s_i} and β_{r_i} where $P_t' = \frac{P_{t-1}+P_{t-2}}{2}$ is the first lag of trailing two-year average cathode price, and β_{GDP} representing the intensity response to regional GDP per capita. For more details see Dr. Fu's thesis.[32]

The resulting regional sectoral demand values were then converted to regional demand by shape (e.g. copper or alloyed wire or tube) using global parameters based on data from Glöser et al.,[46] which permitted distinction between alloyed and unalloyed products, including refined copper use at the global scale. Unalloyed products were assumed on average >99.8% Cu by mass, while alloyed product compositions were determined based on Copper Development Association (CDA) supplier databases and industry expert interviews as described in Supplementary Methods: Semi-Fabricator Alloy Distribution Framework. As such, alloyed semi-fabricator production was broken into 190 representative Unified Numbering System (UNS) alloys, noting European Committee for Standardization (CEN) equivalents.[53-55] It was assumed that the overall distribution of alloying elements within each shape remains constant over time, and consequently the fraction of each shape occupied by each alloy was held constant for each year of production. Since each sector is composed of different fractions of each shape, and that sectors evolve independently as shown in equation 1, demand for individual alloys does not, however, remain constant. Alloy compositional requirements across eight impurity elements were considered for the blending component of the linear programming optimization model described in the following section.

Scrap generation was broken down into 14 categories representing the most common Institute of Scrap Recycling Industries (ISRI) post-consumer scrap grades and 191 categories representing post-industrial scrap produced by alloyed semi-fabricators, with 190 categories representing alloyed post-industrial scrap as described and the single additional alloy representing unalloyed post-industrial scrap. Annual post-consumer scrap generation values for China and the rest of the world were calculated using standard dynamic material flow analysis methods with lognormal sectoral lifetime distributions,[46] with sectoral collection rates and recycling efficiencies for both regions. Refined metals were assumed to be sufficiently liquid to permit any quantity to be consumed at the same unit price globally, but given availability concerns associated with post-consumer scrap consumption, post-consumer scrap prices were determined using an order book formulation, where average purchasing prices increased with total quantities consumed within each region. Given that inventories were sufficiently large that each scrap grade was not fully consumed each year, this formulation permitted an increase in regional scrap availability in a given year to produce an increase in scrap consumption in that region. The resulting equations describing scrap prices relative to quantities consumed were formulated for each scrap grade as functions of scrap availability and scrap price, which was determined using econometric time series analysis. Following the assumption that scrap markets are illiquid, scrap prices were allowed to change based on regional supply-demand imbalances. Additional details surrounding order book, scrap price formation, and additional data for scrap generation are described in Supplementary Methods: Scrap Price Availability, and their Interplay.

With regional manufacturer production and scrap availability determined at the compositional level, a linear programming optimization model was developed within Gurobi Optimization software, where composition constraints were imposed and price was minimized.[56] This model was constrained to consume the quantity of refined copper determined at the global level above, with the distribution between China and the rest of the world a product of scrap and refined metal prices as determined by the optimization model (see Supplementary Methods: Linear Programming Optimization Model).

COVID-19 Pandemic-Centered System Shocks

The range of scenarios explored here reflects the uncertainty surrounding the potential market impacts of COVID-19, including cases of supply surplus and deficit. The 2020 projected 4% decrease in GDP per capita produced a year-over-year decrease in refined copper demand of 2.3% (sensitivities gave 0.6% to 4.1%, Figure 5b), well aligned with projections from Roskill (3-4% decrease),[57] ICSG (4% decrease),[58] and S&P Global (2.4% decrease).[28] Using ICSG's January-May 2019-2020 mining capacity utilization decrease of 2.6% (sensitivity 1.3% to 3.9%), the model produced a mining production decrease of 2.3% (sensitivities gave 1.2% increase to 5.7% decrease), which aligns with projections from ICSG (3% decrease)[27,58] and approximately encompasses that of GlobalData (1.9% increase).[59] Following ICSG data, refinery capacity utilization and secondary ratio were set to decrease 2.3% (1.1-3.4%) and 6.9% (3.5-10%) respectively 2019-2020, resulting in refined production increasing 0.43% year over year (sensitivities gave 1.6% increase to 0.75% decrease). Primary refining production then increases 3.1-3.6% while secondary refining production decreases 5.6-14%. ICSG projected 2020 global refining production to remain unchanged from 2019, with a significant decline in secondary refining production due to the disruption of scrap collection and trade.[27]

From these changes across 48 scenarios with GDP alterations, the average 2019-2020 (2020-2021 due to model temporal resolution) change in cathode price was a decrease of 7.2% with standard deviation of 4.9%. Among the 16 scenarios with limited GDP/capita reduction (2.0%), the average 2020-2021 change in cathode price was a decrease of 2.3% with standard deviation 2.7% (not significantly different from zero), where scenarios with moderate to large changes in refining production generated cathode price changes above zero and reaching as high as 3.2%. Cathode prices are expected to increase up to 10%

from 2020-2021 (2021-2022 in this model) due to the global economic recovery and consequent resurgent demand;[28] our model projects a mean increase of 5.4% with standard deviation 7.9%. When scenarios without changes in mining are omitted, this value increases to 8.2% with standard deviation 6.8% among 63 scenarios. Larger price recovery coincides with increased shock size across all parameters.

Copper cathode price remains high, with the post-recovery average price (2022 to 2040) for the mean of our scenarios 2.4% above the 2019 price. These high prices incentivize primary refining and mining production, leading to a redistribution of primary and secondary refining production – a decrease in scrap consumption and increase in concentrate consumption – while suppressing cumulative total refining production (Figure 5c). Larger reductions in GDP per capita limit the cathode price rebound, mitigating this redistribution and the corresponding rebound in CO_2e emissions (Figure 5d). The mean cumulative decrease in CO_2e emissions produced by 2040 is 33 Mt (13% of 2020 value) with standard deviation 49 Mt (19% of 2020 value). With low GDP shocks excluded, this emissions reduction increases to 58 Mt (23% of 2020 value) with standard deviation 33 Mt (13% of 2020 value) among 32 scenarios. Impacts on the material system are shown in Supplementary Figures S14-S15.

Life Cycle Analysis

This work was primarily performed using the Ecoinvent 3 database within the software package SimaPro, using the environmental damage indicators offered by the Tool for the Reduction and Assessment of Chemical and other Environmental Impacts (TRACI) 2.1 midpoint life cycle inventory analysis method (LCIA), which provides the following ten damage categories: Ozone depletion (kg CFC-kk), Global warming (kg CO2 eq), Smog (kg O3 eq), Acidification (kg SO2 eq), Eutrophication (kg N eq), Carcinogenics (CTUh), Non carcinogenics (CTUh), Respiratory effects (kg PM2.5 eq), Ecotoxicity (CTUe), Fossil fuel depletion (MJ surplus).[60] We also considered total energy consumption using Cumulative Energy

Demand V1.11[61] and water use following Berger et al.[62] For mines, we calculated CO_2e emissions, water use, and energy consumption as a function of ore grade according to relationships established by Northey et al.[63] Average regional ore grades for concentrate and solvent extraction-electrowinning (SX-EW) mines were calculated using SNL data, average regional CO_2e emissions, water use, and energy consumption were calculated following equation (2), and the resulting values were multiplied by regional scaling factors (Supplementary Table S10) to reach the regional values from Ecoinvent 3, TRACI 2.1, Cumulative Energy Demand V1.11, and Berger et al (Supplementary Table 11).

$$C = Ag^B \quad (2)$$

Where C is the calculated impact for the category applied, A and B are empirically-determined constants (Supplementary Table 12), and g is the calculated average ore grade for that region (Supplementary Table 13). This process was used to calculate the emissions or consumption for each mine individually, where the remaining 9 TRACI indicators were calculated based on the ratio of CO_2e emissions to each indicator for the respective region.

Direct melt impacts were calculated by using an equal combination of “treatment of used copper cable” and “treatment of aluminum scrap, post-consumer, prepared for recycling, at remelter” from Ecoinvent 3 inventories, then scaling the resulting values to match literature CO_2e emission values from Giurco et al.[64] Secondary refining impacts were similarly treated, using “treatment of copper scrap by electrolytic refining” and “treatment of used copper cable,” then scaling all indicators to match literature CO_2e emission values from Chen et al.[65] Due to the uncertainty in these values, they were treated as global and applied equally to all direct melt scrap and secondary refining (Supplementary Table 14). Primary refining was calculated using the difference between “market for copper” and copper mining impacts within each indicator analyzed here (Supplementary Table 15). Fabrication was treated using “metal working” within Ecoinvent 3, which was reported for Europe and RoW. The impacts associated with Europe were used for North America in this study as well (Supplementary Table 16). Refined metal use was similarly attributed, using global impacts associated with each alloying element considered here summed with impacts from directly melting No.1 scrap (Supplementary Table 17). Regional distributions within RoW for each of these impact categories were assumed to remain constant at the 2017 levels for each of the years evaluated in this study (Supplementary Table 18).

Competing Interests

The authors declare no competing interests.

References

1 Elshkaki, A., Graedel, T., Ciacci, L. & Reck, B. K. Copper demand, supply, and associated energy use to 2050. *Global environmental change* **39**, 305-315 (2016).

2 Northey, S., Mohr, S., Mudd, G. M., Weng, Z. & Giurco, D. Modelling future copper ore grade decline based on a detailed assessment of copper resources and mining. *Resources, Conservation and Recycling* **83**, 190-201 (2014).

3 Azapagic, A. Developing a framework for sustainable development indicators for the mining and minerals industry. *Journal of cleaner production* **12**, 639-662 (2004).

4 Andreoni, V. & Miola, A. Climate change and supply-chain vulnerability. *International Journal of Emergency Services* (2015).

5 Northey, S. A. *et al.* The exposure of global base metal resources to water criticality, scarcity and climate change. *Global Environmental Change* **44**, 109-124 (2017).

6 Lieder, M. & Rashid, A. Towards circular economy implementation: a comprehensive review in context of manufacturing industry. *Journal of cleaner production* **115**, 36-51 (2016).

7 Geng, Y., Sarkis, J. & Ulgiati, S. Sustainability, well-being, and the circular economy in China and worldwide. *Science* **6278**, 73-76 (2016).

8 Gregson, N. & Crang, M. Made in China and the new world of secondary resource recovery. *Environment and Planning A: Economy and Space* **51**, 1031-1040 (2019).

9 Xia, Y. China's Environmental Campaign: How China's War on Pollution Is Transforming the International Trade in Waste. *NYU Journal of International Law and Politics* **51**, 1101 (2018).

10 Greenstone, M. Four years after declaring war on pollution, China is winning. *New York Times*, A8 (2018).

11 Parker, L. China's ban on trash imports shifts waste crisis to Southeast Asia. *National Geographic. Available at: www. nationalgeographic. com/environment/2018/11/china-ban-plastic-trash-imports-shifts-waste-crisis-southeast-asia-malaysia (accessed 22 May 2019)* (2018).

12 Ren, Y., Shi, L., Bardow, A., Geyer, R. & Suh, S. Life-cycle environmental implications of China's ban on post-consumer plastics import. *Resources, Conservation and Recycling* **156**, 104699 (2020).

13 Sun, N. & Phoonphongphiphat, A. China's scrap plastic ban saddles neighbors with piles of problems. *Nikkei Asian Review Online* (2018).

14 Staub, C. Policies drive Chinese processing investments across the globe. *Resource Recycling, Inc.* (2018).

15 Staub, C. Details on upcoming U.S. recycling projects from Chinese firms. *Resource Recycling, Inc.* (2018).

16 Lee, J., Wei, S.-J. & Xu, J. Trade Surplus, Heavy Imports, and Pollution. (2019).

17 Brooks, A. L., Wang, S. & Jambeck, J. R. The Chinese import ban and its impact on global plastic waste trade. *Science advances* **4**, eaat0131 (2018).

18 Huang, Q. *et al.* Modelling the global impact of China's ban on plastic waste imports. *Resources, Conservation and Recycling* **154**, 104607 (2020).

19 Zeng, X., Ali, S. H., Tian, J. & Li, J. Mapping anthropogenic mineral generation in China and its implications for a circular economy. *Nature communications* **11**, 1-9 (2020).

20 Wang, J., Ju, Y., Wang, M. & Li, X. Scenario analysis of the recycled copper supply in China considering the recycling efficiency rate and waste import regulations. *Resources, Conservation and Recycling* **146**, 580-589 (2019).

21 Qu, S. *et al.* Implications of China's foreign waste ban on the global circular economy. *Resources, Conservation and Recycling* **144**, 252-255 (2019).

22 Dong, D. *et al.* Scenarios for anthropogenic copper demand and supply in China: implications of a scrap import ban and a circular economy transition. *Resources, Conservation and Recycling* **161**, 104943 (2020).

23 MacDonald, A. *COVID-19 mining impacts — Impact to mine sites winding down*, <https://platform.mi.spglobal.com/web/client?auth=inherit#news/article?id=58535277&KeyProductLinkType=4> (2020).

24 Rutland, T. *Copper CBS May 2020 — COVID-19 supply disruptions offset demand shortfalls*, <https://platform.mi.spglobal.com/web/client?auth=inherit#news/article?id=58485894&KeyProductLinkType=4> (2020).

25 Laing, T. The economic impact of the Coronavirus 2019 (Covid-2019): Implications for the mining industry. *The Extractive Industries and Society* (2020).

26 Newman, L. *Copper price surges due to global shortage*, <https://www.aljazeera.com/news/2020/07/copper-price-surges-due-global-shortage-200701163458731.html> (2020).

27 The Impact of the COVID-19 Pandemic on World Copper Supply. (International Copper Study Group, 2020).

28 Sappor, J. *et al. COVID-19 impacts — Metals price recovery fragile as recession concerns loom*, <https://platform.mi.spglobal.com/web/client?auth=inherit&overridecdc=1&#news/article?id=59221008&KeyProductLinkType=23> (2020).

29 Ivanov, D. Predicting the impacts of epidemic outbreaks on global supply chains: A simulation-based analysis on the coronavirus outbreak (COVID-19/SARS-CoV-2) case. *Transportation Research Part E: Logistics and Transportation Review* **136**, 101922 (2020).

30 Maffioli, E. M. How Is the World Responding to the Novel Coronavirus Disease (COVID-19) Compared with the 2014 West African Ebola Epidemic? The Importance of China as a Player in the Global Economy. *The American Journal of Tropical Medicine and Hygiene* **102**, 924-925 (2020).

31 Gupta, M. *et al.* COVID-19 and economy. *Dermatologic therapy* (2020).

32 Fu, X. *Assessing Byproduct Mining and Metal Recycling as Indicators of Material Criticality* Doctoral thesis, Massachusetts Institute of Technology, (2019).

33 Daly, T. & Zhang, M. *China publishes new standards for copper and aluminum scrap*, <https://www.reuters.com/article/us-china-metals-scrap/china-publishes-new-standards-for-copper-and-aluminum-scrap-idUSKBN1ZI0IA> (2020).

34 Home, A. *Column: How China is upending copper scrap and why it matters*, <https://uk.reuters.com/article/uk-china-copper-scrap-ahome/column-how-china-is-upending-copper-scrap-and-why-it-matters-idUKKCN1RM1VV> (2019).

35 *The standard rules for recycled brass raw materials, recycled copper raw materials, and recycled cast aluminum alloy raw materials have been announced*, <https://news.smm.cn/news/101019061> (2020).

36 *Greenhouse Gas Emissions from a Typical Passenger Vehicle*, <https://www.epa.gov/greenvehicles/greenhouse-gas-emissions-typical-passenger-vehicle> (2018).

37 Basov, V. *The Chinese scramble to mine Africa*, <https://www.mining.com/feature-chinas-scramble-for-africa/> (2015).

38 World Economic Outlook, April 2020: The Great Lockdown. (International Monetary Fund, 2020).

39 Laurence, D. in *Proceedings of the First International Seminar on Mine Closure.* 83-94 (Australian Centre for Geomechanics).

40 *Mine closure impact on global copper supply – report*, <https://www.mining.com/mine-closures-pose-risk-to-global-copper-supply-report/> (2020).

41 Eheliyagoda, D. *et al.* Examining the Temporal Demand and Sustainability of Copper in China. *Environmental Science & Technology* **53**, 13812-13821 (2019).

42 Liu, S. *et al.* Recycling the domestic copper scrap to address the China's copper sustainability. *Journal of Materials Research and Technology* (2020).

43 Ayres, R. U., Ayres, L. W. & Råde, I. *The life cycle of copper, its co-products and byproducts*. Vol. 13 (Springer Science & Business Media, 2003).

44 Aklin, M. Re-exploring the trade and environment nexus through the diffusion of pollution. *Environmental and Resource Economics* **64**, 663-682 (2016).

45 Bhuwalka, K., Swei, O., Roth, R. & Kirchain, R. Estimating Copper Price Elasticity using Bayesian Hierarchical Modeling. (Under Preparation).

46 Glöser, S., Soulier, M. & Tercero Espinoza, L. A. Dynamic analysis of global copper flows. Global stocks, postconsumer material flows, recycling indicators, and uncertainty evaluation. *Environmental Science and Technology* **47**, 6564-6572 (2013).

47 China Copper Market Study. *Shanghai Metals Market* (2019).

48 World Copper Factbook 2018. (International Copper Study Group, 2018).

49 ICSG 2018 Statistical Yearbook. (International Copper Study Group, 2018).

50 International World Copper Council. *Global Semis Production and Demand*, <http://www.coppercouncil.org/iwcc-statistics-and-data> (2020).

51 S&P Global Market Intelligence. *SNL Metals & Mining Data* (2019).

52 UN Comtrade Database. *UN Comtrade Online* (2019).

53 European Committee for Standardization. (European Committee for Standardization, 2015).

54 Copper Development Association. *Copper and Copper Alloys: Compositions, Applications & Properties*, 2004).

55 Society of Automobile Engineers. *Unified Numbering System for Copper and Copper Alloys*, <http://unscopperalloys.org/> (2020).

56 Gurobi Optimizer Reference Manual (2020).

57 Kinch, D. *Metals demand outperforming GDP metrics, copper leads way - Roskill*, <https://www.spglobal.com/platts/en/market-insights/latest-news/metals/082720-metals-demand-outperforming-gdp-metrics-copper-leads-way-roskill> (2020).

58 *Selected Data*, <https://www.icsg.org/index.php/statistics/selected-data> (2020).

59 *Copper production will still grow in 2020, says GlobalData*, <https://www.mining-journal.com/copper-news/news/1384164/copper-production-will-still-grow-in-2020-says-globaldata> (2020).

60 Bare, J. Tool for the reduction and assessment of chemical and other environmental impacts TRACI 2.1: User's manual. United States Environmental Protection Agency, SOP No. (S-10637-OP-1-0, 2012).

61 Frischknecht, R. *et al.* (Citeseer, 2007).

62 Berger, M., van der Ent, R., Eisner, S., Bach, V. & Finkbeiner, M. Water accounting and vulnerability evaluation (WAVE): considering atmospheric evaporation recycling and the risk of freshwater depletion in water footprinting. *Environmental science & technology* **48**, 4521-4528 (2014).

63 Northey, S., Haque, N. & Mudd, G. Using sustainability reporting to assess the environmental footprint of copper mining. *Journal of Cleaner Production* **40**, 118-128 (2013).

64 Giurco, D., Stewart, M., Suljada, T. & Petrie, J. Copper recycling alternatives: an environmental analysis. *Proceedings of the 5th annual environmental engineering research event, Noosa, Australia*, 20-23 (2006).

65 Chen, J. *et al.* Environmental benefits of secondary copper from primary copper based on life cycle assessment in China. *Resources, Conservation and Recycling* **146**, 35-44 (2019).

Figures

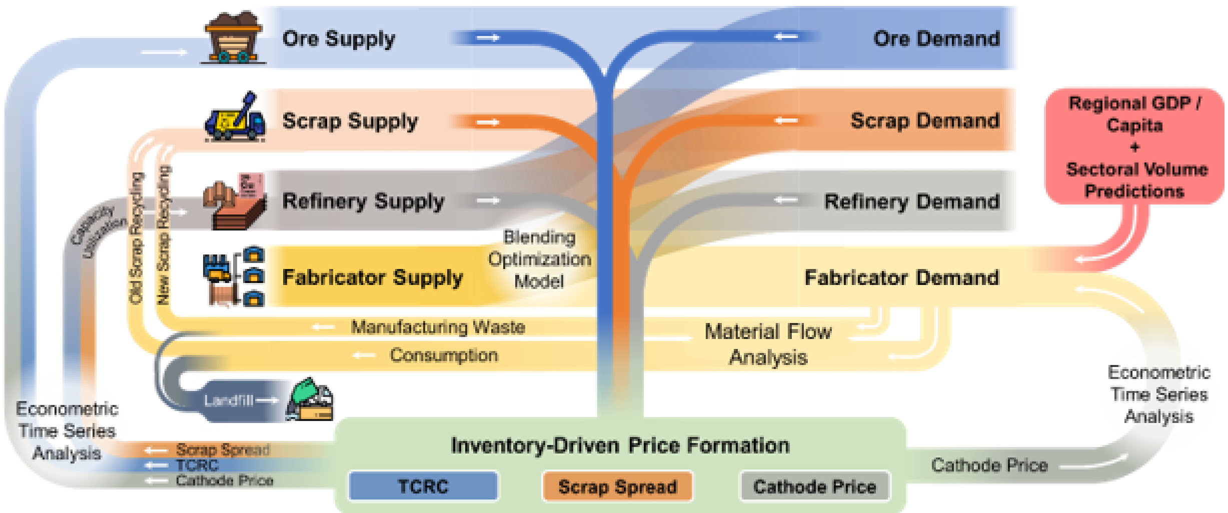

Figure 1

Model architecture. Supply-demand imbalances for copper ore, scrap, and cathode are used to calculate TCRC, scrap spread, and cathode price evolution, respectively, using inventory-driven price formation. Several of these supply-demand modules are linked; for example, refinery production (supply) uses both copper ore and scrap as raw materials and therefore determines demand for those materials. Likewise, fabricator production determines refined copper cathode and scrap demand through the blending optimization model. With prices formed, econometric time series analysis permits calculation of mine and refinery production evolution. Fabricator demand (consumption of copper) is determined using both cathode price and the exogenous variables gross domestic product (GDP) per capita and sectoral volume predictions. Fabricator demand permits calculation of scrap generation via material flow analysis. The resulting imbalances among these variables permit evolution year over year.

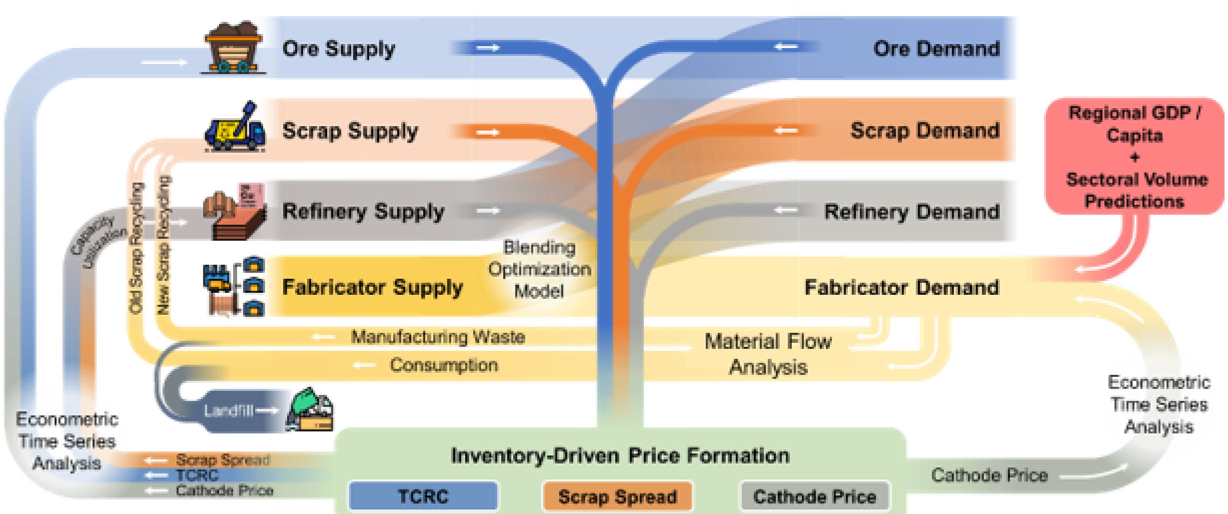

Figure 1

Model architecture. Supply-demand imbalances for copper ore, scrap, and cathode are used to calculate TCRC, scrap spread, and cathode price evolution, respectively, using inventory-driven price formation. Several of these supply-demand modules are linked; for example, refinery production (supply) uses both copper ore and scrap as raw materials and therefore determines demand for those materials. Likewise, fabricator production determines refined copper cathode and scrap demand through the blending optimization model. With prices formed, econometric time series analysis permits calculation of mine and refinery production evolution. Fabricator demand (consumption of copper) is determined using both cathode price and the exogenous variables gross domestic product (GDP) per capita and sectoral volume predictions. Fabricator demand permits calculation of scrap generation via material flow analysis. The resulting imbalances among these variables permit evolution year over year.

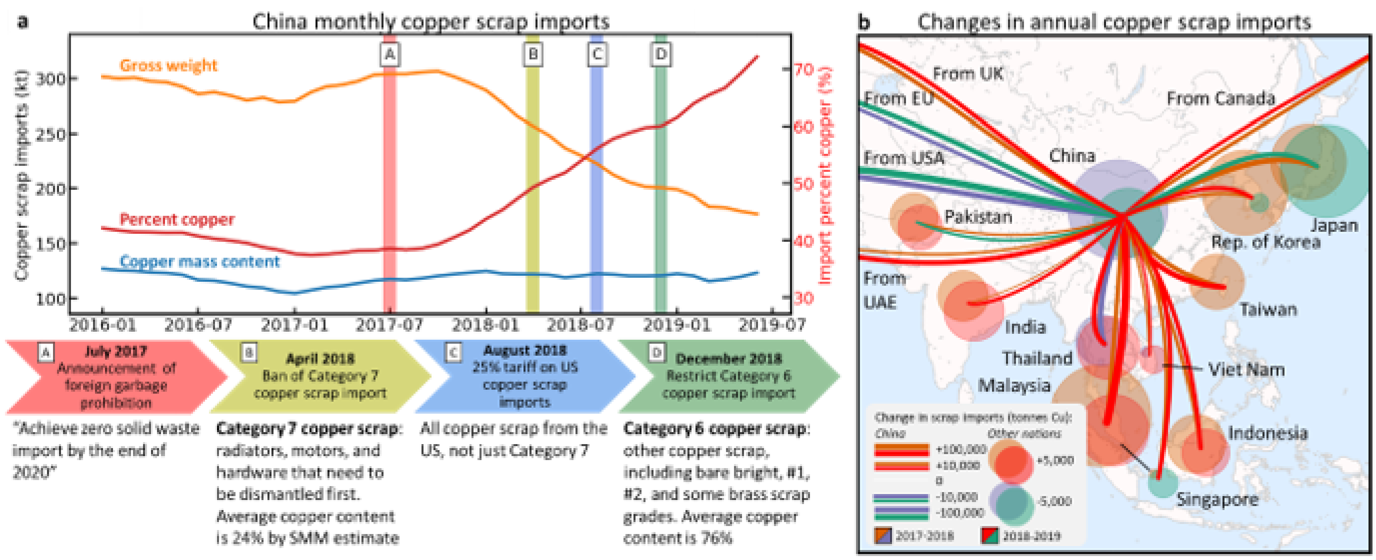

Figure 2

Changes in monthly and annual copper scrap imports for China and surrounding region. a, China's scrap-related policy actions and the consequent decrease in gross weight scrap imports, increase in the percent copper or copper fraction of those imports, and the near-constant resulting copper mass content. b, Changes in the copper content of copper scrap imports for countries surrounding China and their exports to China, where year-over-year increases are shown in orange (2017-2018) and red (2018-2019), while decreases are shown in blue (2017-2018) and green (2018-2019). Bubbles represent changes in the corresponding country's copper imports, while lines represent changes in that country's exports to China. Note: The designations employed and the presentation of the material on this map do not imply the expression of any opinion whatsoever on the part of Research Square concerning the legal status of any country, territory, city or area or of its authorities, or concerning the delimitation of its frontiers or boundaries. This map has been provided by the authors.

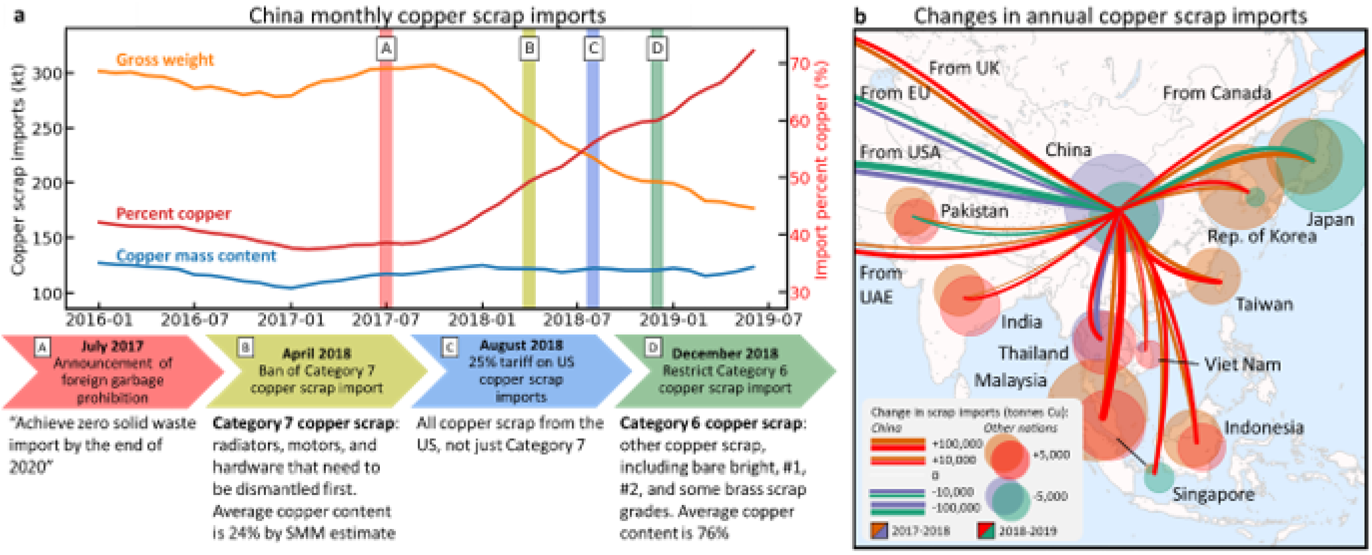

Figure 2

Changes in monthly and annual copper scrap imports for China and surrounding region. a, China's scrap-related policy actions and the consequent decrease in gross weight scrap imports, increase in the percent copper or copper fraction of those imports, and the near-constant resulting copper mass content. b, Changes in the copper content of copper scrap imports for countries surrounding China and their exports to China, where year-over-year increases are shown in orange (2017-2018) and red (2018-2019), while decreases are shown in blue (2017-2018) and green (2018-2019). Bubbles represent changes in the corresponding country's copper imports, while lines represent changes in that country's exports to China. Note: The designations employed and the presentation of the material on this map do not imply the expression of any opinion whatsoever on the part of Research Square concerning the legal status of any country, territory, city or area or of its authorities, or concerning the delimitation of its frontiers or boundaries. This map has been provided by the authors.

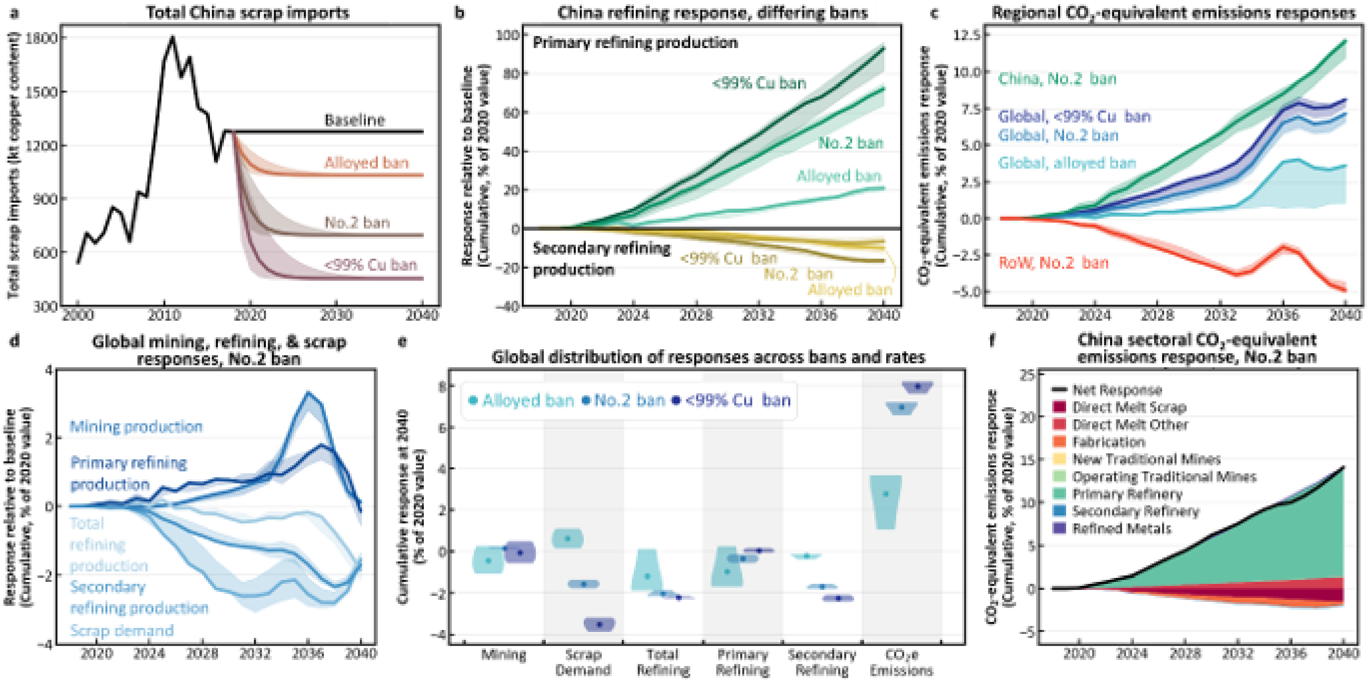

Figure 3

System response for China's solid waste import ban, No.2 ban with additional emphasis. In each subfigure, the shading surrounding solid lines corresponds to the variation in ban rate: 25, 50, or 75% year over year, where solid lines represent a 50% year-over-year ban of the listed scrap type. a, Scrap imports for each scenario in copper content. b, Cumulative primary and secondary refining responses in China relative to baseline for each scenario using total refining production as reference. c, Cumulative regional CO2e emissions responses for each scenario at the global level and regional results for the No.2 scrap ban over the simulation period. Global values are used as divisors for regional parameters for ease of comparison. d, Cumulative global mining, refining, and scrap demand responses for the No.2 scrap ban over the simulation period. Labels correspond with relative positions of their values at 2040. e, The distributions of global mining, scrap demand, total refining, primary refining, secondary refining, and CO2e emissions responses for each ban, evaluated cumulatively at 2040 relative to baseline. Points represent the mean of the three ban rates, while the shaded regions represent the distributions of ban rate results. f, Cumulative sectoral CO2e emissions response for China, where all increasing impacts were plotted above the x-axis, all decreasing impacts were plotted below the x-axis, and the black line represents the net response within China as a result of these sectoral changes.

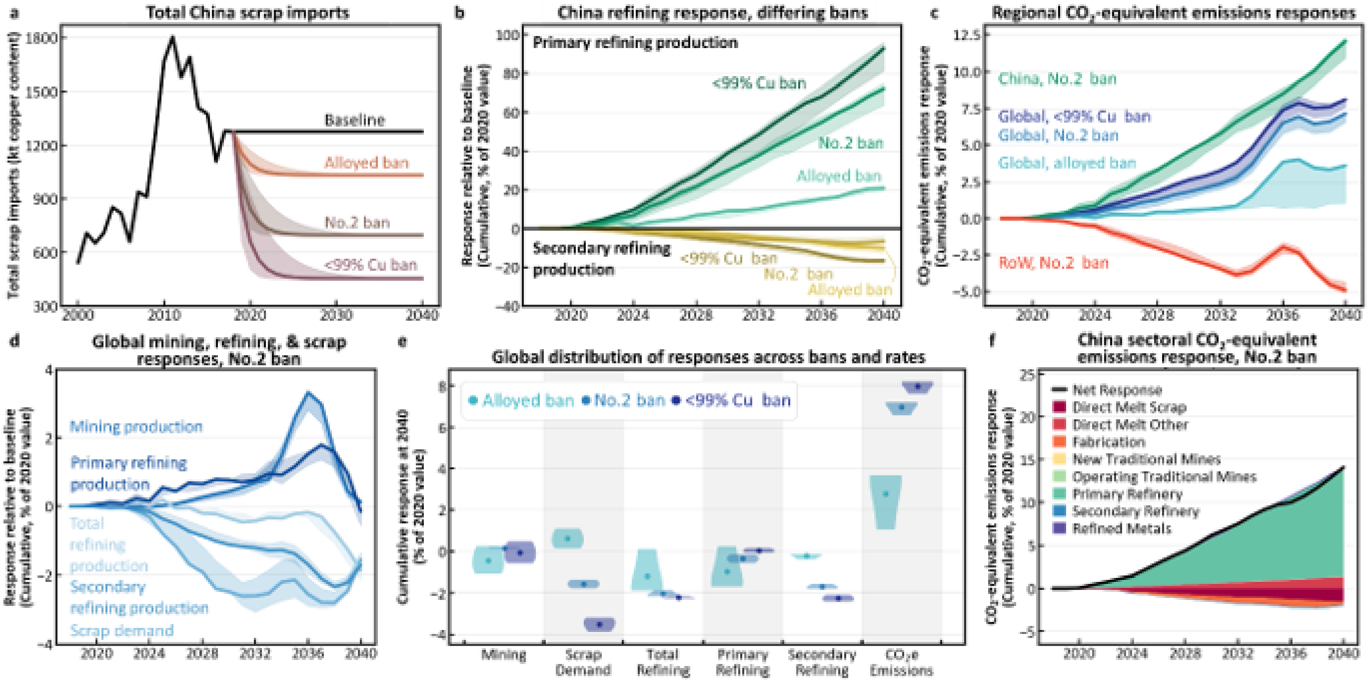

Figure 3

System response for China's solid waste import ban, No.2 ban with additional emphasis. In each subfigure, the shading surrounding solid lines corresponds to the variation in ban rate: 25, 50, or 75% year over year, where solid lines represent a 50% year-over-year ban of the listed scrap type. a, Scrap imports for each scenario in copper content. b, Cumulative primary and secondary refining responses in China relative to baseline for each scenario using total refining production as reference. c, Cumulative regional CO2e emissions responses for each scenario at the global level and regional results for the No.2 scrap ban over the simulation period. Global values are used as divisors for regional parameters for ease of comparison. d, Cumulative global mining, refining, and scrap demand responses for the No.2 scrap ban over the simulation period. Labels correspond with relative positions of their values at 2040. e, The distributions of global mining, scrap demand, total refining, primary refining, secondary refining, and CO2e emissions responses for each ban, evaluated cumulatively at 2040 relative to baseline. Points represent the mean of the three ban rates, while the shaded regions represent the distributions of ban rate results. f, Cumulative sectoral CO2e emissions response for China, where all increasing impacts were plotted above the x-axis, all decreasing impacts were plotted below the x-axis, and the black line represents the net response within China as a result of these sectoral changes.

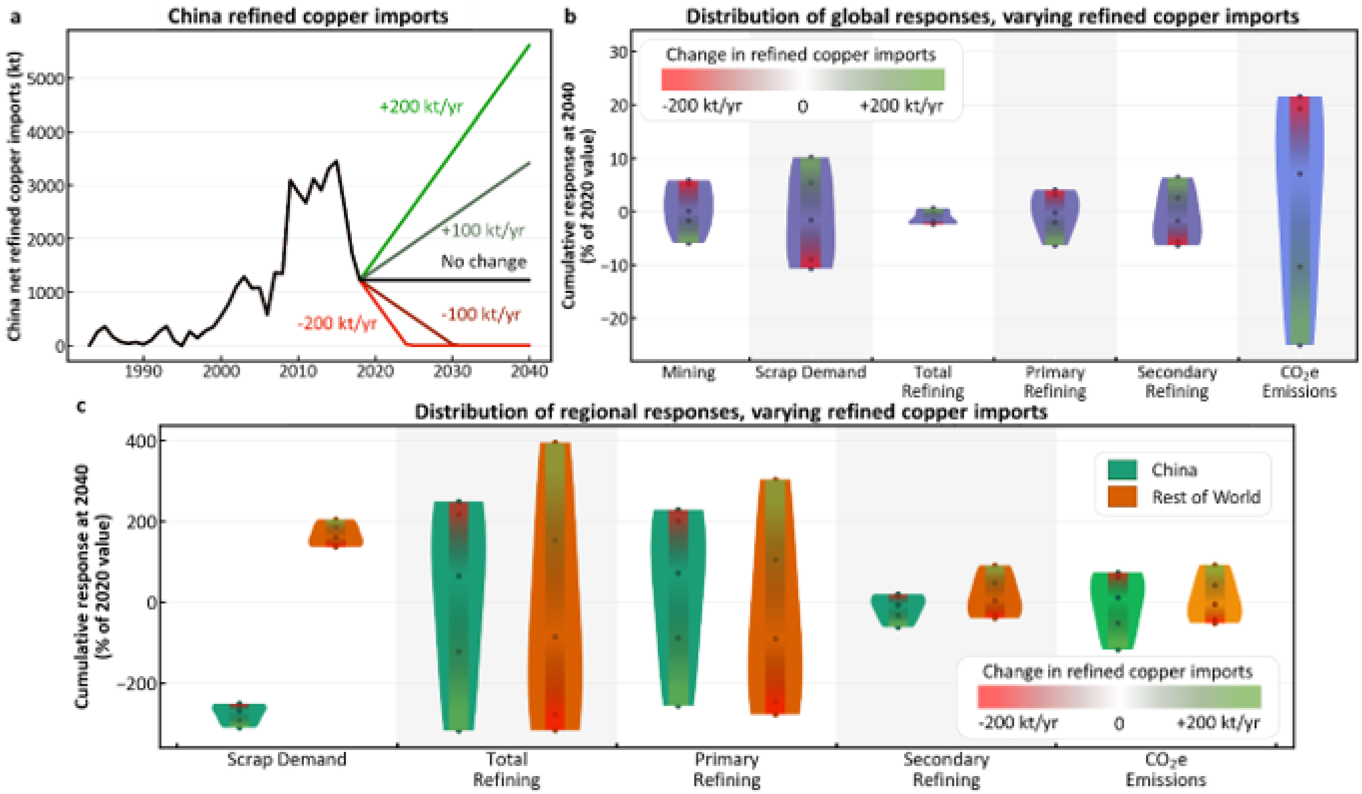

Figure 4

Results of changing China's refined copper imports under condition of No.2 scrap ban. a, Historical Chinese net refined copper imports and scenario definition, where refined copper imports are increased or decreased at rates of 100 or 200 kt/year, with minimum value zero. b, Violin plot showing the distributions of global responses for varying refined copper imports, where CO2e emissions are highlighted as an aggregate response. c, Violin plot showing the distributions of regional responses for each supply chain actor, with CO2e emissions highlighted as a system-level response. China is shown in green, the rest of world in orange. CO¬2e emissions use the global value as divisor for ease of comparison; the extrema using local divisors are China: -270% and 170%, RoW: -120% and 210%. Primary, secondary, and total refining use the global or regional total refining value as divisor.

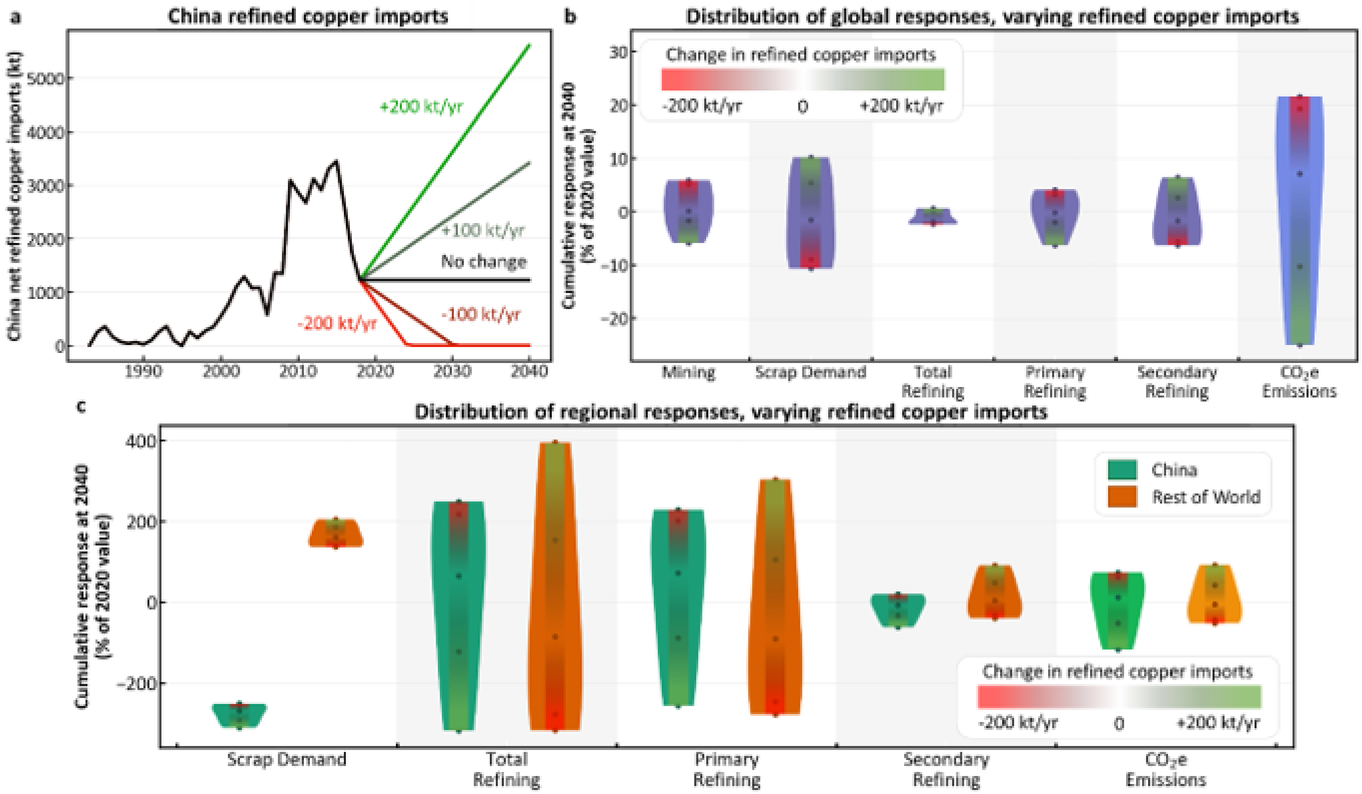

Figure 4

Results of changing China's refined copper imports under condition of No.2 scrap ban. a, Historical Chinese net refined copper imports and scenario definition, where refined copper imports are increased or decreased at rates of 100 or 200 kt/year, with minimum value zero. b, Violin plot showing the distributions of global responses for varying refined copper imports, where CO2e emissions are highlighted as an aggregate response. c, Violin plot showing the distributions of regional responses for each supply chain actor, with CO2e emissions highlighted as a system-level response. China is shown in green, the rest of world in orange. CO¬2e emissions use the global value as divisor for ease of comparison; the extrema using local divisors are China: -270% and 170%, RoW: -120% and 210%. Primary, secondary, and total refining use the global or regional total refining value as divisor.

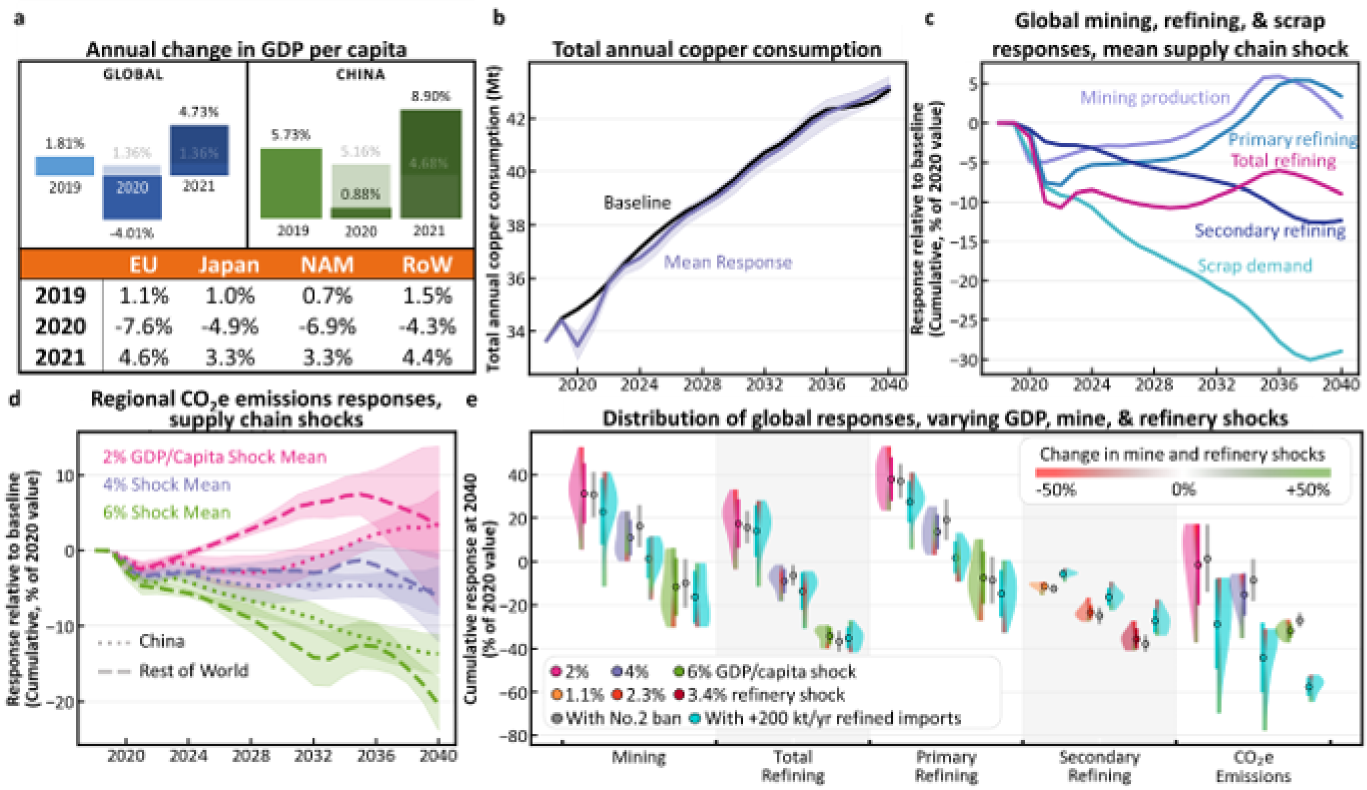

Figure 5

System response to COVID-19 scenarios and supply chain disruption sensitivities. a, The annual changes in GDP per capita for 2019, 2020, and 2021 used in the COVID-19 response scenario, using values adapted from annual change in GDP from the International Monetary Fund. Baseline values for China and global are shown in gray. b, Global annual copper consumption including alloyed and unalloyed refined and scrap copper consumption for baseline and the mean COVID-19 scenario response. Shaded areas represent one standard deviation. c, Cumulative global secondary refining, scrap demand, mining production, total refining, and primary refining responses relative to baseline as a percent of the 2020 value, labelled from top to bottom using 2040 as reference. Standard deviations not shown for clarity. d, Cumulative CO2e emissions responses relative to baseline for China and RoW as a percent of the 2020 global value. e, Violin plot showing the distribution of global responses for COVID-19 response scenarios using 2, 4, and 6% declines in global GDP per capita from 2019-2020, with mean values shown as same-colored points. Gray points and bars represent the mean system response and standard deviation when the No.2 scrap China solid waste import ban is simulated simultaneous with the COVID-19 shocks. Green and red bars indicate the magnitude of the mine and refinery system shocks. For secondary refining, GDP changes produced near-equal violin plots and here the data are grouped by the three levels of refinery shock instead.

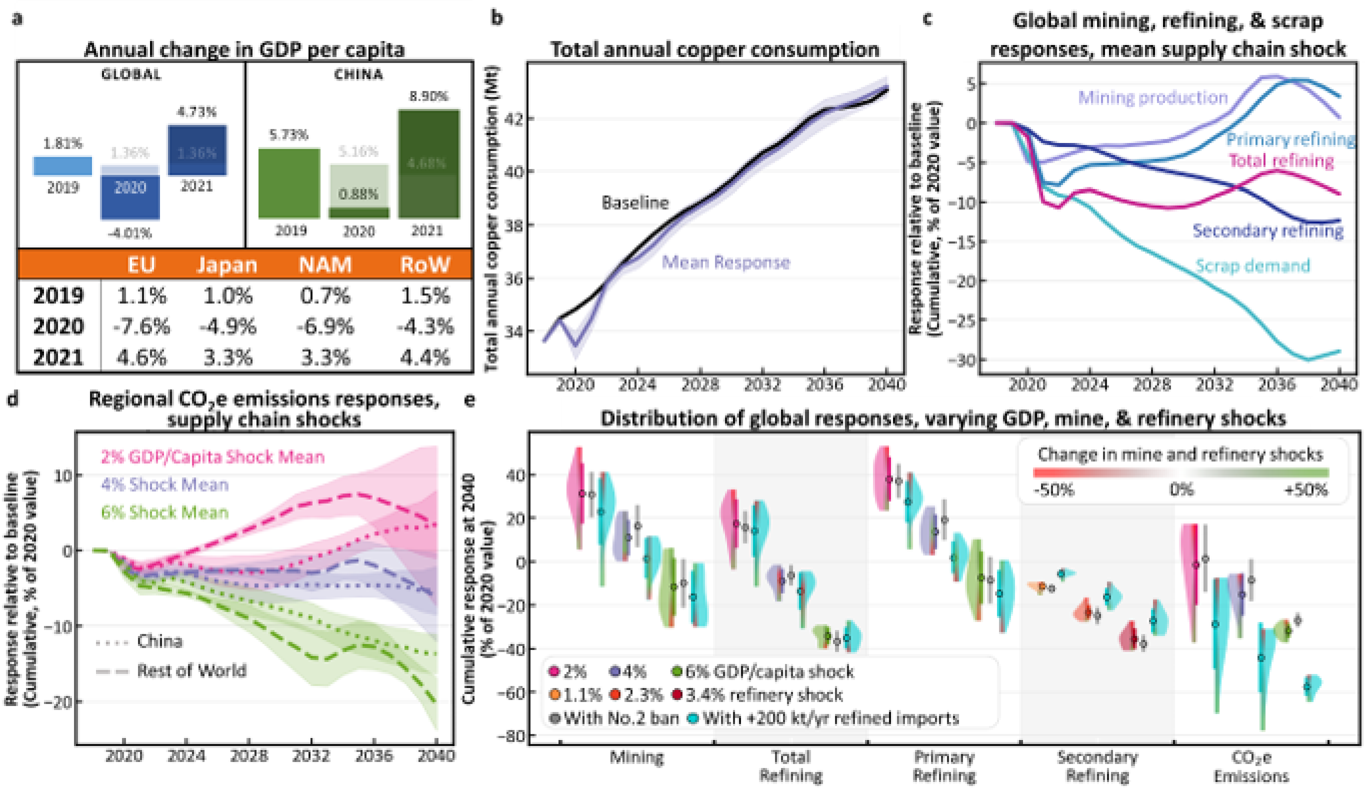

Figure 5

System response to COVID-19 scenarios and supply chain disruption sensitivities. a, The annual changes in GDP per capita for 2019, 2020, and 2021 used in the COVID-19 response scenario, using values adapted from annual change in GDP from the International Monetary Fund. Baseline values for China and global are shown in gray. b, Global annual copper consumption including alloyed and unalloyed refined and scrap copper consumption for baseline and the mean COVID-19 scenario response. Shaded areas represent one standard deviation. c, Cumulative global secondary refining, scrap demand, mining production, total refining, and primary refining responses relative to baseline as a percent of the 2020 value, labelled from top to bottom using 2040 as reference. Standard deviations not shown for clarity. d, Cumulative CO2e emissions responses relative to baseline for China and RoW as a percent of the 2020 global value. e, Violin plot showing the distribution of global responses for COVID-19 response scenarios using 2, 4, and 6% declines in global GDP per capita from 2019-2020, with mean values shown as same-colored points. Gray points and bars represent the mean system response and standard deviation when the No.2 scrap China solid waste import ban is simulated simultaneous with the COVID-19 shocks. Green and red bars indicate the magnitude of the mine and refinery system shocks. For secondary refining, GDP changes produced near-equal violin plots and here the data are grouped by the three levels of refinery shock instead.

Supplementary Files

This is a list of supplementary files associated with this preprint. Click to download.

- ChinaSupplementaryInformation.docx
- ChinaSupplementaryInformation.docx
- ChinaTableS19.xlsx
- ChinaTableS19.xlsx